MS Thesis Report

Phenomenological Modeling of Soot Process in Diesel Engine Combustion

Author

Fozul Azeem Baig

MS-ME-12

Reg # NUST201260438MSMME62212F

Thesis Supervisor

Dr. Samiur Rahman Shah (SMME)

GEC members

- Dr. Shahid Ikramullah Butt (SMME)
- Dr. Riaz Ahmad Mufti (SMME)
- Dr. Muhammad Sajid (SMME)

Table of Contents

Abstract

During the last two decades, several emission standards have been implemented all over the world defining the permissible values of the pollutants. As a result, pollution reduction has become a major problem for the researchers in the field of internal combustion engines. Although diesel engines are considered more efficient than gasoline engines for their power, better fuel economy and less CO_2 emissions, but the major concern is the high emitted level of Nitrogen oxides (NOx) and particulate matter (PM).

In Europe, the Euro standards are being used which set different levels of nitrous oxides (NOx) and particulate matter (PM) for the diesel engines.

The Euro 6 standard allows PM levels upto 0.005g/km. For achieving this small value a lot of effort has been put up nowadays for reducing the emissions. For diesel engines, the after treatment reduction of emissions using NOx traps and selective catalytic reduction (SCR) are expensive and difficult to implement. Therefore, at source reduction techniques have been developed, the most common of which is exhaust gas recirculation (EGR).

Water injection (WI), by different means i.e. either by a separate injector in the chamber, by mixing with the fuel or injecting in the manifold is also used for decreasing NOx by dropping the combustion chamber temperature.

This research has been performed to model the soot process in a diesel engine. Soot is the carbon based solid element and is a major component of PM. For this purpose, a simulation model of a diesel engine is developed which leads to soot production. By changing the parameters such as speed, air to fuel ratio, injection timing etc, soot production can be predicted using this model. Moreover, a modification in the model has been made to incorporate EGR and WI in the model to see the behavior of the soot process. The simulated results are then compared with the experimental results, with and without the emission reduction techniques.

The soot formation model show satisfactory agreement with the experimentally measured values which results in the validation of this model as a soot prediction tool. The modification in the model also shows good results with the measured results with EGR and WI at different loading conditions.

1. Introduction to diesel engine combustion

Although diesel engines are considered more efficient than gasoline engines for their power, better fuel economy and less CO_2 emissions, but the major concern is the high emitted level of Nitrogen oxides (NOx) and soot. Therefore emission modeling has always been of vital role for diesel industry. Soot is one of the major emissions in diesel combustion and its chemistry is the most complex to understand. Soot modeling is now gaining more significance as the legislation has put very strict limitations on this emission.

Before going into the details of soot formation, diesel engine combustion need to be understood. In a diesel engine, two types of combustion take place i.e.

1. Pre-mixed combustion
2. Mixing-controlled combustion or Diffusion combustion

For better explanation, the rate of heat release diagram for a DI diesel engine is shown in fig. 1 [2] and a fuel jet is shown in fig. 2 [34].

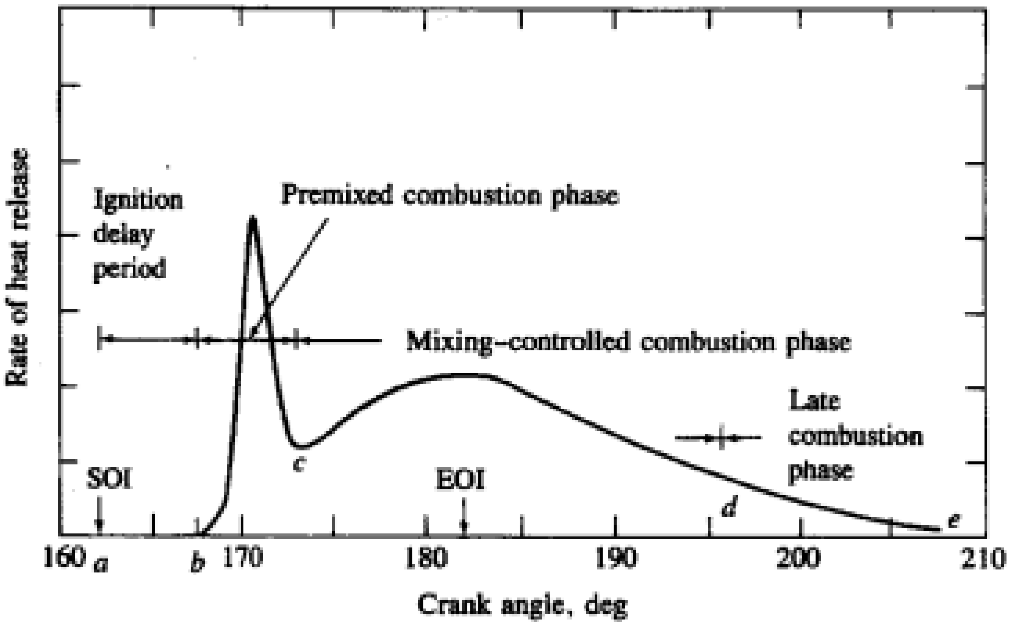

Fig. 01. DI Diesel engine heat-release rate diagram[2]

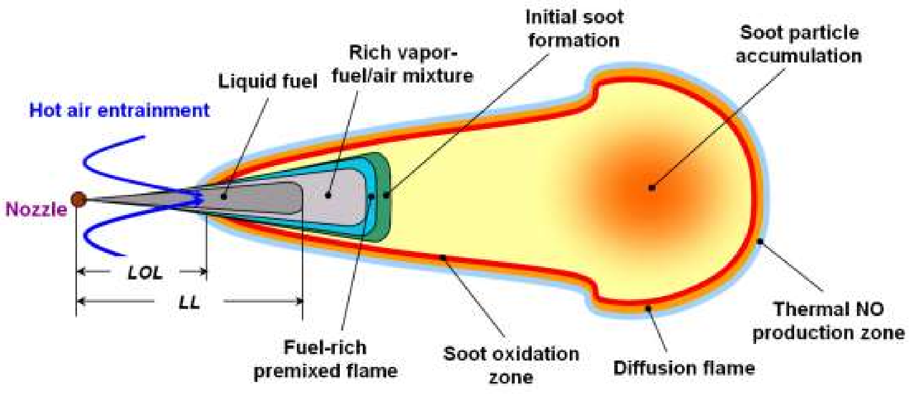

Fig. 02. Schematic representation of diesel spray jet [34]

In figure 1, SOI is the start of injection and EOI is the end of injection. Four different stages of combustion are shown which are explained below:

a→ At this point, fuel with high pressure and velocity is injected into the heated air charge in the chamber. This fuel, upon meeting with the air, starts to atomize due to high temperature and collision with the air molecules. This aids in better mixing of the fuel droplets with the air. Furthermore, evaporation of the fuel droplets takes place and an air/fuel mixture thus starts to form. This mixture starts to move away from the injector core. At a certain point downstream of the nozzle the evaporation process completes. The maximum length to which the fuel remains in liquid state is known as liquid length (LL) as shown in fig. 2 [34]. The high temperature helps in the mixing reaction. Up to this point the combustion has not yet started and this time is referred as ignition delay shown as a to b in the figure. The temperature of the air/fuel mixture is about 700K to 800K. [33]

b→ Auto ignition takes place and all the accumulated air/fuel mixture burns rapidly releasing a high amount of heat energy and the temperature in the chamber suddenly rises to about 1400K to 1600K [33]. This is shown in the first half of b to c. The other half shows that after the initial burning the intensity is reduced and the heat level drops. This phase between points a and c represents the pre-mix combustion phase. During this phase, the conditions are ideal for soot formation i.e high temperature and lack of oxygen. This will be discussed in detail in the next sections.

c→ From this point the mixing-controlled or diffusion combustion phase starts. The rate of heat release and the duration of burning are controlled by the injected fuel. This phase of combustion continues up to point d shown in the figure. The remaining chemical energy of the fuel is released here and temperatures of 2500K to 2700K are achieved [33]. Due to high velocity of the fuel jet coming from the nozzle, the diffusion flame is formed at a certain distance from the injector nozzle known as lift-off length (LOL) as shown in fig. 2.

d→ At this point, the injection of fuel has been stopped and is referred as late combustion phase shown from d to e in the fig 1. The unburned fuel and fuel rich combustion products are burned here but at a very slow rate as the temperature of the chamber has dropped due to the start of the expansion stroke.

The flame jet with temperatures and combustion products in different zones is shown in fig. 3 [33]

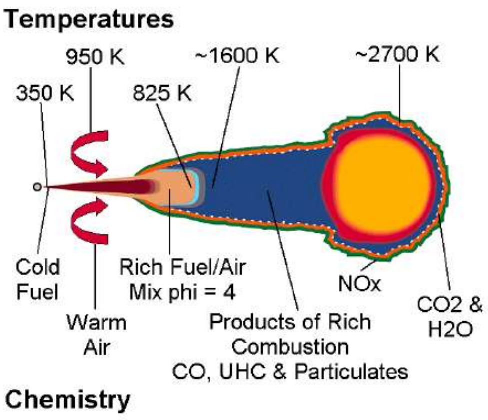

Fig. 03. Evolution of temperature and combustion products in the flame jet[33]

The time based evolution of the fuel jet is shown in fig. 4 [33]

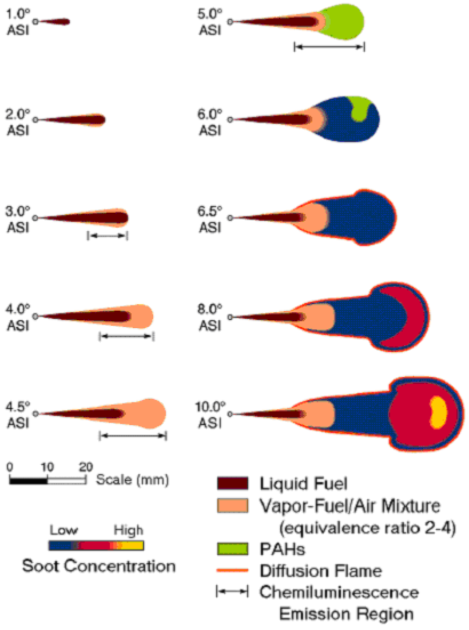

Fig. 04. Development of fuel jet from injection to combustion[33]

The above figure shows the development of the fuel jet after the injection of fuel. In the left four frames the air/fuel mixture generation is shown which increase with time forming an envelope around the fuel jet. The right four frames show the development of combustion products which mainly includes short chain hydrocarbons which further aids in the soot production explained in the next section.

2. Soot Production Phenomena

The soot formed during combustion cannot be chemically or physically defined uniquely. It is quite different from graphite and black in color with majority portion made up of carbon. In a soot particle, hydrogen is present which is bonded to the carbon atoms. The amount of hydrogen depends on the time taken for the combustion to happen. The particles which spend more time in the combustion environment contain low amounts of hydrogen. The density of soot is about 1.8 g/cm^3.

The particulate matter emissions (PM) from a diesel engine constitutes of soot and soluble organic fractions (SOF). Soot is the carbonaceous and insoluble part of the total PM [30]. The net soot production, which includes both formation and oxidation is a combination of the following, partially parallel processes.[30]

1. Fuel pyrolysis
2. Particle nucleation
3. Surface growth
4. Coalescence and agglomeration
5. Oxidation

The schematic of soot formation is shown in fig. 5 [31] below.

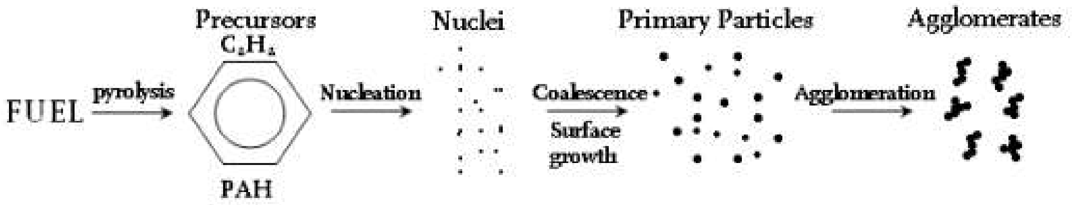

Fig. 05. Schematic of phenomenology of soot formation process [31]

2.1. Fuel Pyrolysis

In this process, a change in structure happens due to heat without oxidation. This process is dependent on the concentrations of reactants and temperature. Pyrolysis is responsible for the generation of soot precursors. [25] During combustion, there happens a competition between the pyrolytic reactions and the oxidation rate as both these processes are temperature dependant. With increase in temperature, the oxidation process tends to speed up as compared to pyrolysis. Thus the net soot production remains less in both premixed and diffusion flames when temperature is increased. As a result of pyrolysis, polycyclic aromatic hydrocarbons (PAH), acetylene (C_2H_2) and unsaturated hydrocarbons are produced.

2.2. Nucleation

The addition of small units particularly C_2H_2, is responsible for the growth of the first aromatic ring which further turns into PAH. The mass keeps on adding and the molecular structure is changed to particles. These particles are very small in size but provide sites for the soot growth which increases the net soot mass. Nucleation mainly happens near the initial reaction zone where the temperatures and reactant concentrations are high.

2.3. Surface growth

The major mass to the soot particles is added during this process. So the time during which surface growth happens is very critical in the production of the final soot. The mass of the soot particles is increased by the addition of the gas phase hydrocarbons to the small soot particles. The growth species form a bond with the soot particles resulting in the growth of particle size. The number of particles during this phase remains the same when they move down stream of the initial reaction zone.

2.4. Coalescence and Agglomeration

The combination of particles happens during these processes. Unlike surface growth, the number of particles does not remain the same; rather they decrease in number while keeping the mass constant.

During coalescence, two particles combine to form a single large particle whereas in agglomeration two particles stick together to form a chain like structure in which each particle has its own individual structure.

2.5. Oxidation

It is only process by which there is a decrease in the net soot production. The conversion of HC to CO, CO_2 and H_2O is termed as oxidation. The formation of CO indicates that the carbon has been partially oxidized, thus it does not affect the soot formation. As reviewed by Tree & Svensson [31], when the temperature in the chamber reaches above 1300K the soot oxidation takes place. OH radicals are also responsible for oxidation in rich and stoichiometric conditions. [31].

3. Combustion Models

The combustion models are divided into four categories depending on the computation and complexity involved. [30]

1. Empirical models
2. Semi-empirical model
3. Phenomenological models
4. Physical combustion models

3.1. Empirical models

Pure empirical correlations are used in this model. These models are prone to error outside the operating conditions. More errors occur if extrapolation is used.

3.2. Semi-empirical model

This model involves inputs taken from the experimental data. This data is then used for solving rate equations which lead to soot formation. Experience of the model developer has a vital role in this type.

3.3. Phenomenological models

The physics and chemistry of combustion is involved in this type of model. The variables can be calculated using simple but macroscopically physical based models.[30]. In comparison to semi-empirical models, these models can be used outside the operating range and extrapolation can be used. The rate of heat release (ROHR) and emission formation can be predicted using these models.

3.4. Physical combustion models

The highest level of details in involved in these models regarding the physical and chemical process occurring during the combustion. The chamber is divided into small cells and equations of conservation of mass, momentum and energy are solved for each cell. Therefore such models are the most accurate for emission prediction but involves high computing power.

4. Emission Reduction Techniques

Although many at source and after source emission reduction techniques are in practice nowadays, our main focus shall remain on exhaust gas recirculation (EGR) and water injection (WI) and its effects on the soot production. These two techniques are briefly discussed below in light of different research works done in this regard.

4.1. Exhaust Gas Recirculation (EGR)

In this technique, exhaust gas around 15% to 20% [1] is routed back in the intake manifold which results in the dilution of the fresh air entering the cylinder. The fresh air is displaced with carbondioxide and water vapors. Thus the amount of oxygen in the air decreases which has a negative effect on the combustion. The burning does not remain stable and the peak temperature drops. This substantially reduces the NO concentrations. [2]

The %EGR is the quantity of recirculated exhaust by mass introduced in the total intake mixture i.e.

$$\%EGR = \frac{Intake\ air\ mass\ with\ EGR}{Intake\ air\ mass} \times 100$$

Desantes [13] used CO_2 concentrations in their measurements to define the %EGR using the CO_2 in the atmosphere, at the exhaust and the intake manifold. The relation is as follows.

$$\%EGR = \frac{|CO_2|_{intake} - |CO_2|_{atm}}{|CO_2|_{exhaust} - |CO_2|_{atm}}$$

The total exhaust from an engine equipped with EGR is low as a part of it is routed back in the engine. [2] Thus the amount of toxic matter drops for the same volumetric concentration of exhaust.

Ken Satoh et al [3] performed experiments on a naturally aspirated diesel engine with different amounts of EGR and variation of other parameters and found that NOx concentration has a direct proportion with the oxygen level in the cylinder. But it has an adverse effect on the smoke production. This is because as the average temperature drops along with the oxygen levels, the soot oxidation rate becomes low.

EGR also has a direct relation with the engine loading. At low loads, the amount of carbon dioxide and water vapors being circulated back in the engine is low so a high percentage of EGR can be introduced in the cylinder. The case is opposite for higher loads i.e. the oxygen concentration becomes very low leading to a drop in diffusive combustion and appearance of more soot. [4]

Wagner[14] performed experiments to achieve lower levels of NOx along with the soot emissions. For this purpose, a highly diluted intake mixture was introduced in the chamber with about 44% EGR rate. It was observed that both NOx and PM were decreased but there was a negative impact on the fuel economy. In spark ignition engines with direct injection, introducing exhaust gases improved the fuel economy [15, 16].

Therefore, it can be deduced that introduction of exhaust gases in the engine can lead to negative effects. High soot emissions and high fuel economy are the major penalties that are observed in the diesel engines. So a trade-off between NOx and soot is made when using EGR [17-22]. In case of soot (smoke), more quantity is formed during combustion and less quantity is oxidized or burned, thus increasing the net soot produced at the exhaust. [23]. This increase in the soot has several bad effects on the engine performance such as increased carbon deposits and wear of engine parts such as piston rings, bearings, valve train and cylinder liner. Increase in corrosion and adsorption is observed along with rupture of anti-wear film by soot.[24]

If the charge entering the cylinder is cooled it is referred as cooled EGR. This helps in improving the volumetric efficiency of the engine as the density of the mixture is increased.

4.2. Water Injection

During the Second World War, thrust augmentation in gas turbines was done by injecting water. Water is also used in spark ignition engines for decreasing knock, thus enabling the engine to be operated at high boost pressures and giving high power outputs.[25]

It was then found that the use of water in engines also has the tendency to reduce pollutant emissions particularly NOx emissions. This is because combustion is modified by injecting water in the engine. Therefore, a lot of research is carried out on this topic for engines and turbines. [26]. The main methods of water injection are: [5, 6]

- Water/Fuel Emulsion injection
- Combustion chamber water injection
- Stratified water injection
- Intake manifold water injection

WI is mainly used for NOx reduction but in some case it might tend to reduce the particulate matter as well.[6]. Due to evaporation of the water added in the engine, its dissociation and the increase in the specific heat capacity of the mixture, the temperature in the chamber drops thus reducing the NOx production.

In our case, the water was injected in the intake manifold, therefore our main focus shall remain on this technique, and its effects on the soot production. In this technique, both liquid and vapors of water can be injected in the intake manifold of the engine. If the engine is turbocharged, water maybe injected before or after the compressor. For injection, both single and multiple injectors are used for evenly distribute the water in the cylinder. Injection can be continuous or pulsed when liquid water is used.

One of the advantages of the manifold injection is that same rate of fuel injection can be used. WI can also be used as a complement to EGR for significantly reducing NOx emissions with a better NOx/soot trade-off.[7,8]

Ladommatos [27] performed some experiments on a 2.5 liter diesel engine with direct injection. The engine was kept at 40% load with an air-fuel ratio of 44.6:1. The injection timing was advanced and kept at 10° BTDC. Vapors of water were injected which substituted the oxygen in the air. It was observed that the NOx produced was dropped at 150ppmv from 560ppmv. On the contrary, soot was increased to 5.6g/kg from 2.6g/kg of fuel.

Samec [28] used two different WI systems on a 7.1 litre 4 cylinder DI diesel engine. One system was named "WS1" which injected liquid water in front of each inlet port and the other was named "WS2" which injected water before the compressor. Both systems showed almost similar pollutant (NOx and PM) production rates but a different thermal loading on the engine. Due to the latent heat of vaporization of water, the temperature at cylinder and head was lower with WS1 than WS2. The soot production rate was observed at maximum torque and 1300rpm and is shown in figure 6.

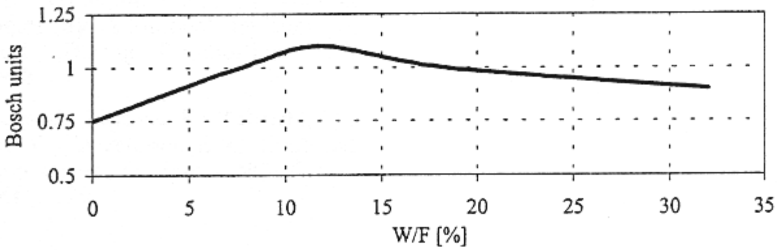

Fig. 06. Variation of Soot production with varying water injection rate [28]

As shown in the above figure, soot production was increased initially possibly due to the decrease in the oxygen available. After a certain water to fuel ratio, the soot production decreased due to reduction in temperature and the burning of injected fuel in premixed combustion.

WI has a cooling effect in the chamber resulting in the reduction of bulk gas temperature and chamber pressure. Due to reduced temperature the soot oxidation rate is affected and the net soot production is increased. OH radicals are produced in the chamber when water is introduced in the engine by the reaction [6]

$$H_2O + O \rightarrow OH + OH$$

$$H_2O + H \rightarrow OH + H_2$$

In the high temperature zones i.e the regions where all oxygen is being consumed and the mixture ratio is close to stoichiometric, the soot oxidation rate is positively assisted by these OH radical and the net soot production decreases.[9] Therefore in comparison with EGR, due to the oxidation enhancement by the OH radicals, WI tends to increase the soot production but not as much as EGR alone.

Keeping in view the above discussion, the major effects of water injection on diesel engine combustion are as follows.

1. Thermal effects
2. Dilution effects
3. Chemical effects

4.2.1. Thermal effects

When liquid water is injected in the inlet manifold, the temperature of the air charge drops due to evaporation. This results in more air available to the fuel due to increase in density of charge with the temperature drop, thus increasing the air mass flow in the engine.

The reduction in temperature causes an increase in the lift-off length, ignition delay, liquid length and the amount of fuel that will burn in the premixed phase. Therefore, the soot production during the premixed combustion phase decreases as noted by Siebers [35].

4.2.2. Dilution effects

The oxygen concentration per unit volume is decreased by the introduction of an inert medium (gas or liquid) in the combustion mixture. Due to this decrease in oxygen, the combustion process slow down and the peak temperature of the flame is dropped which results in the reduction of NOx [9] A greater volume of air charge has to be taken by the fuel jet due to the drop in oxygen levels in the air.

Another effect of dilution is that when the oxygen level in the air charge is reduced, the quantity of soot produced is increased as the oxidation of soot is also reduced

4.2.3. Chemical effects

During combustion heat is generated which results in dissociation of some diluents to form other species that act as pollutant reduction agents. In case of water, H and OH radicals are produced which help in the oxidation of soot thus reducing their quantity. [29]. In case of water vapor addition, Landommatos [27] indicated an increase in the PM emissions by preparing an intake charge which only affects the combustion chemically, and the thermal and dilution effects are negligible.

5. Soot Formation model

In the last few decades, great efforts are being made for the phenomenology that is involved in the formation of soot and its burning. As a result, a better understanding has now been developed for the physics and chemistry of this process but some parts are still debatable. The formation of soot depends on the system and therefore open for more questions.[10]

Soot is mostly carbon, with small amounts of hydrogen and oxygen [10]. It is mainly produced due the incomplete oxidation of hydrocarbons or pyrolysis at high temperature.

Kouremenos [32] developed a model for predicting soot and NO emissions from a relatively complex geometry. The engine used was a single cylinder, swirl prechamber Ricardo engine. The displacement volume was 536cm^3. In both chambers, a two zone model was used for describing the burned and unburned gases. The simple Hiroyasu [11, 12] model was used in their calculation. On comparison of the predicted soot with the measured ones, the results were good to about 20% or better at three different loads. The prediction of NO was not that accurate. This demonstrated that over a limited range of conditions, this model is useful as well as simple.

Therefore, amongst many soot models presented in literature [10], the semi empirical Hiroyasu model [11,12] is used to predict the soot production in the engine. According to this model, the net soot produced in the cylinder is the difference between the soot formation and soot oxidation rates. Both formation and oxidation rates are dependent on the local cylinder pressure and temperature, according to Hiroyasu.

Moreover, the formation rate also depends on the fuel vapor mass and the oxidation rate depends on the partial pressure of oxygen in the mixture and the local soot mass.

Mathematically, the two steps of the model are shown in the equations:

$$\frac{dm_{sf}}{dt} = A_f m_{fv} P^{0.5}\, exp\left(\frac{-E_{sf}}{RT}\right)$$

$$\frac{dm_b}{dt} = A_b m_{sf} \left(\frac{P_{O_2}}{P}\right) P^{1.8}\, exp\left(\frac{-E_b}{RT}\right)$$

$$\frac{dm_{net}}{dt} = \frac{dm_{sf}}{dt} - \frac{dm_b}{dt}$$

Where:

m_{sf} → Mass of soot formation (kg)

A_f , A_b → Pre-exponential constants for soot formation and burning/oxidation respectively (s^{-1})

m_{fv} → Mass of fuel vapor (kg)

P → Local cylinder pressure (bar)

E_{sf}, E_b → Activation energy of formation and burning respectively $\left(\frac{J}{mol}\right)$

m_b → Mass of soot burned/oxidized (kg)

P_{O_2} → Partial pressure of oxygen (bar)

R → Gas constant $\left(\frac{J}{mol.K}\right)$

T → Local cylinder temperature (K)

m_{net} → Net soot mass (kg)

The constants A_f and A_b are empirically adjusted to match experimental data and

$E_{sf} = 8 \times 10^4 \left(\frac{J}{mol}\right)$, [10]

$E_b = 12 \times 10^4 \left(\frac{J}{mol}\right)$ [10]

6. Dilution Ratio

When EGR or water is introduced in the engine the oxygen concentration in the air mixture is decreased. This change in concentration is calculated by measuring the initial and final amounts of oxygen in the air and is termed as dilution ratio (DR), expressed in percentage i.e.

$$DR(\%) = 100 \times \frac{Oxygen_{ini} - Oxygen_{final}}{Oxygen_{ini}}$$

In other words, DR shows the amount by which oxygen is decreased in the air when exhaust gas or water is introduced in the mixture. The more the amount of exhaust gas recirculated or water injected the more the reduction in oxygen and thus a higher dilution of air. So the net soot depends directly on the dilution ratio.

7. Modification in model

To incorporate the effect of dilution ratio, a new factor 'X' was introduced in the soot formation equation of the model i.e.

$$\frac{dm_{sf}'}{dt} = X\frac{dm_{sf}}{dt}$$

X depends directly on the engine load and amount of oxygen being reduced in the mixture and is expressed as:

$$X = N^{*}.T^{*}.\exp\left((n_1 \times DR(\%))^{n_2}\right)$$

Where

$$N^{*} = \frac{1.4 * N}{N''} \qquad T^{*} = \frac{T_{avg}}{T_{max}}$$

T_{max}→ maximum torque that the engine can provide

N''→ optimal engine speed at maximum torque

N→ engine speed (rpm)

T_{avg}→ average torque (N.m)

n_1→ empirical coefficient depending on the BMEP and can be computed from fig 07.

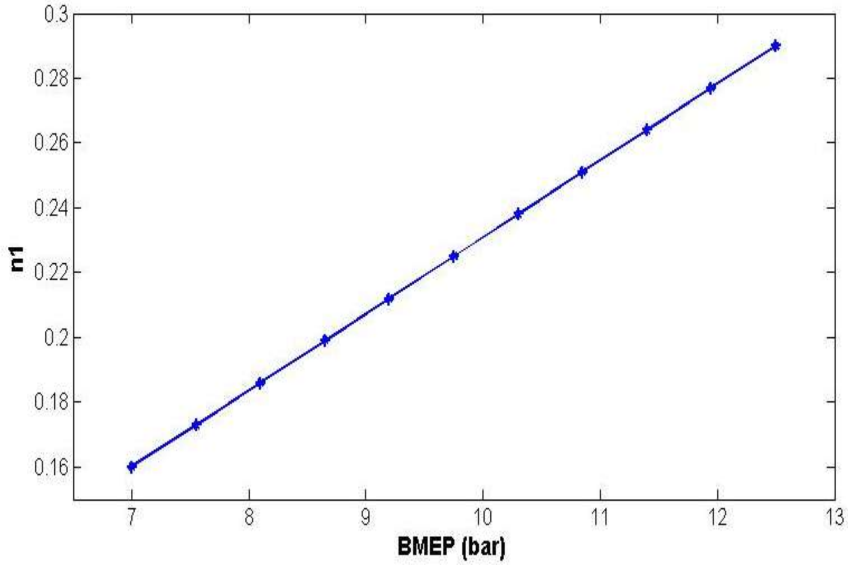

Fig. 07. Computation of n_1 from BMEP

n_2→ empirical power coefficient and its value can be taken from table 01.

Table 01: Values of n_2

	n_2
EGR	1
EGR+WI	0.85
WI	1,0.7*

* if, $(\frac{\dot{m_w}}{\dot{m_f}})$<1, n_2= 1, else n_2= 0.7.

$\dot{m_w}$ → water flow rate (kg/h)

$\dot{m_f}$ → fuel flow rate (kg/h)

8. Engine Specifications

The engine selected is a four stroke inline 4-cylinder diesel engine. Other specifications are given in table 02:

Table 02: Test engine specifications

Displacement	1998cc
Bore	85mm
Stroke	88mm
Connecting rod length	152mm
Compression ratio	18:1
Valves/cylinder	4
EGR system	High pressure, Cooled EGR
Maximum Power	100kW @ 4000rpm
Maximum Torque	320Nm @ 1750rpm

9. Test Points

To validate the model, the tests were performed on the engine at three different loading conditions (A,B,C) to have a better idea of the behavior of soot at the exhaust. Some parameters are as follows:

Table 03: Engine parameters at different load points

Parameters	Test Points		
	A	**B**	**C**
Engine speed (rpm)	1511	1662	1995
Avg. Torque (N.m)	42	107	197
Fuel flow (kg/h)	2.1	4.8	9.6
Air flow (kg/h)	96.3	111	185
Soot measured at exhaust (g/h)	0.246	0.526	1.7

10. Results and Discussion

After applying the selected Hiroyasu model the net soot formation rate was computed. The measured pressure curve was used and the other parameters were determined using the test data. The net soot at the exhaust was calculated by integrating the soot curve obtained by the model as shown in fig, 7.

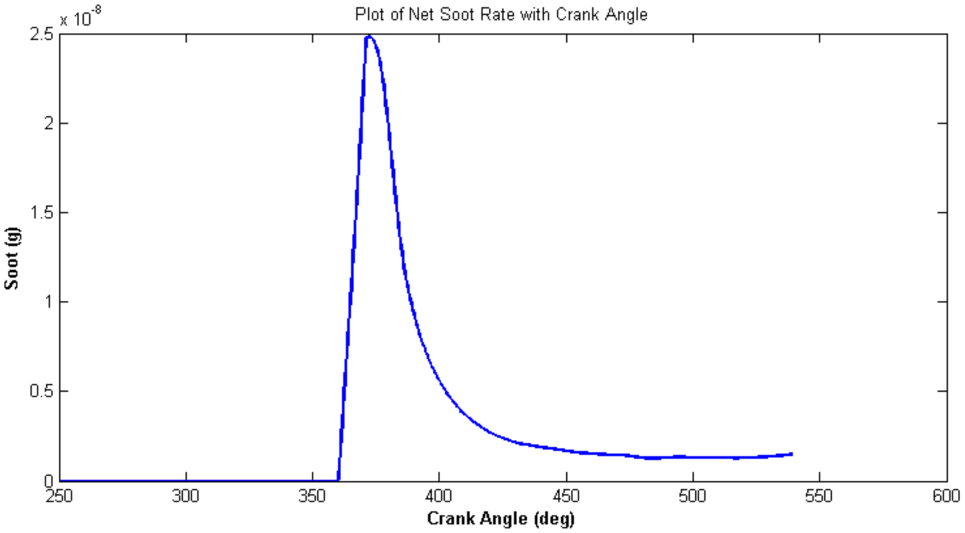

Fig. 08. Soot quantity with crank angle at point C

On comparison with the experimental data, the model showed good results at all the load points as shown in fig. 8.

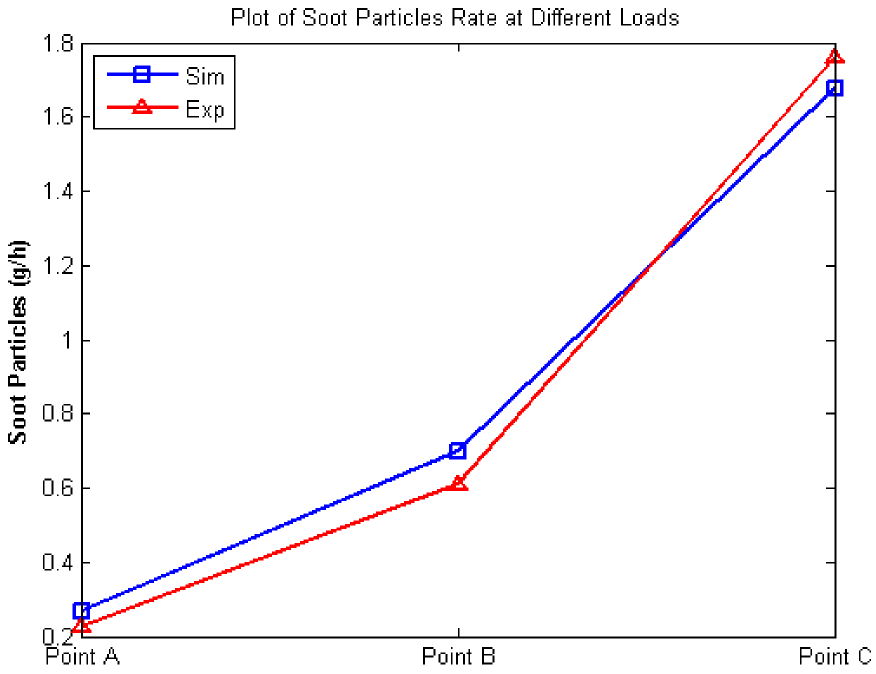

Fig. 09. Comparison of simulated and measured results at A, B and C

So the simulated model showed convincing results after comparison with the experimental data and also showed its versatility at different loads. The next step is to see the behavior of the model when exhaust gas is introduced in the engine.

$A_f = 7.5 \times 10^{-3}\ s^{-1} \qquad A_b = 5 \times 10^{-4}\ s^{-1}$

10.1. Results with EGR without the modification

The tests were performed with different dilution ratios at point B and C as shown in table 04:

Table 04: Dilution ratios at point B and C

Test Point	Diution Ratio (%)			
B	5.14	8.6	12.595	15.912
C	1.65	4.18	6.76	8.089

On comparing the simulated results of EGR at point C with the experimental ones the model showed large errors as shown in fig. 9.

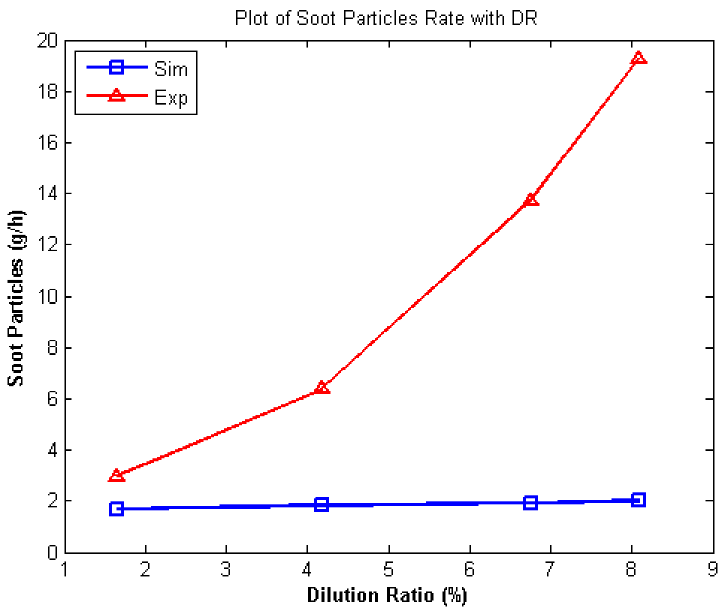

Fig. 10. Comparison of simulated and measured results with EGR at point C without modification

10.2. Results with EGR after modification in model

After the modification in the model the results were plotted and it was found that the simulated and the measured results showed very good agreement with each other. The results for the net soot rate with the dilution ratios for point B and C are shown in fig 11 and fig 12 respectively.

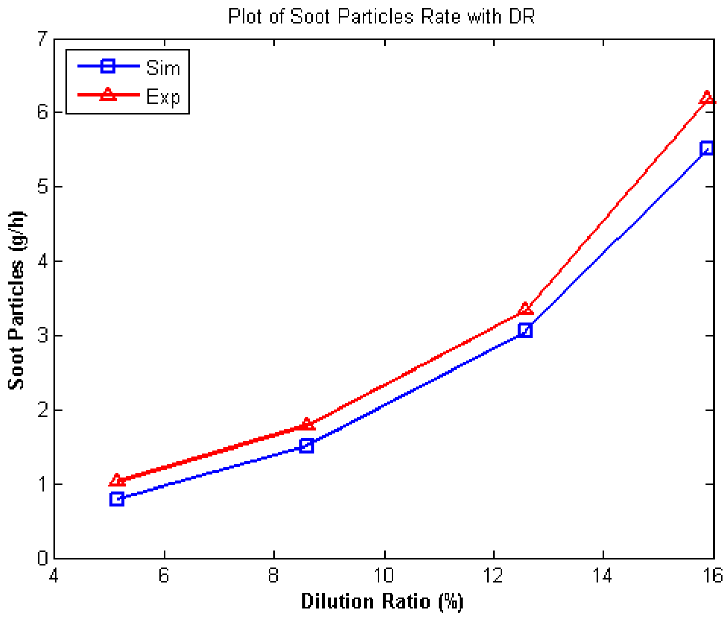

Fig. 11. Comparison of simulated and measured results with EGR at point B after model modification

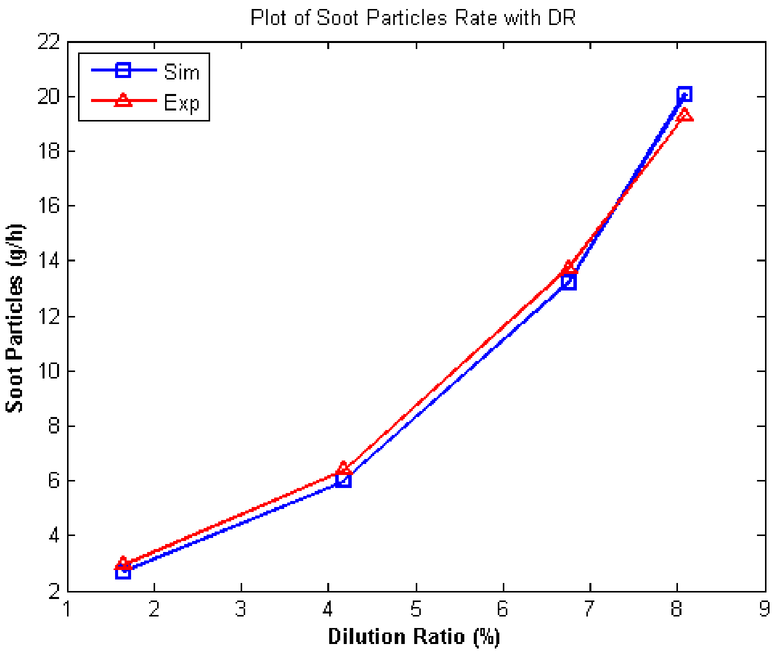

Fig. 12. Comparison of simulated and measured results with EGR at point C after model modification

The soot plots with crank angle at different dilution ratios for test point C are shown in fig. 13.

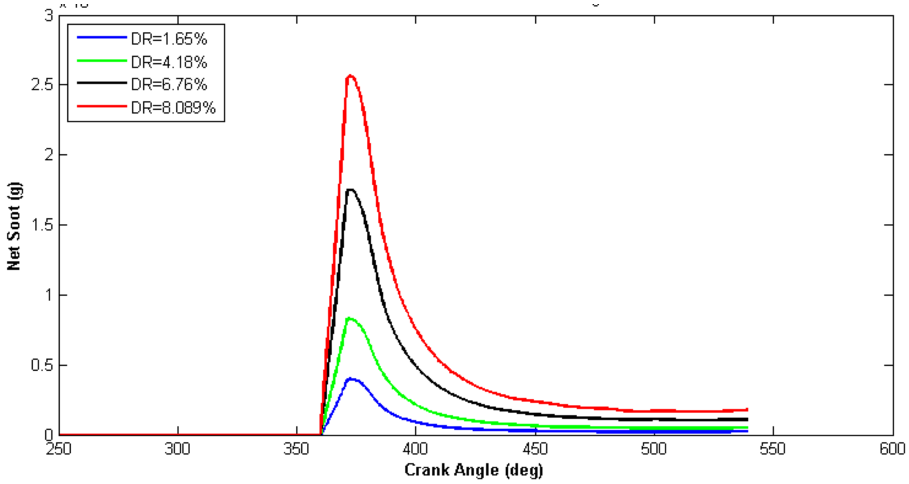

Fig. 13. Soot quantity with crank angle at different dilution ratios at point C

The measured and simulated values at point B and C for different dilution ratios are shown in table 05.

Table 05: Soot value comparison at point B and C for EGR

Test Point	DR (%)	Measured Soot (g/h)	Simulated Soot (g/h)
B	5.14	1.033	0.798
	8.6	1.782	1.507
	12.595	3.339	3.057
	15.912	6.188	5.51
C	1.65	2.96	2.68
	4.18	6.4	6
	6.76	13.74	13.21
	8.089	19.26	20.04

10.3. Results with EGR and Water

The amount of water injected and the dilution ratios for points B and C are shown in table 06.

Table 06: Dilution ratios and amount of water at point B and C

Test Point	DR (%)	$\dot{m}_w$ (g/h)	m_w (mg)
B	5.298	3	15.1
	9.039	3	15.3
	12.867	3	15.1
	17.063	3	15.5
C	4.875	6	24.7
	7.018	6	24.2
	8.957	6	24.9
	10.419	6	24.5

In this case for both points, the ratio $(\frac{\dot{m}_w}{\dot{m}_f})$ remains less than 1 so the value of n_2 used is also 1. After applying the same modified model for this case where both exhaust gas and water is injected in the cylinder the results were plotted. The simulated graphs again showed reasonable accuracy with the measured results. The main difference was seen at point B where the engine load is relatively lower than point C. It was seen that as the DR was increased the error also increased. This error is probably due to the low temperature combustion that happened due to the introduction of water. Therefore the actual net soot produced was lower whereas the simulated results showed a higher side of net soot. The error was less at point C as there was proper combustion happening due to more fuel and air being injected. The results for net soot for point B and C are shown in fig 14 and fig. 15 respectively. The results at point B and C with EGR and WI for different dilution ratios are shown in table 07.

Table 07: Soot value comparison at point B and C for EGR+WI

Test Point	DR (%)	Measured Soot (g/h)	Simulated Soot (g/h)
B	5.298	0.666	0.804
	9.039	1.196	1.428
	12.867	2.134	2.556
	17.063	3.565	4.51
C	4.875	9.755	9.302
	7.018	15.393	15.451
	8.957	24.851	23.329
	10.419	33.341	31.907

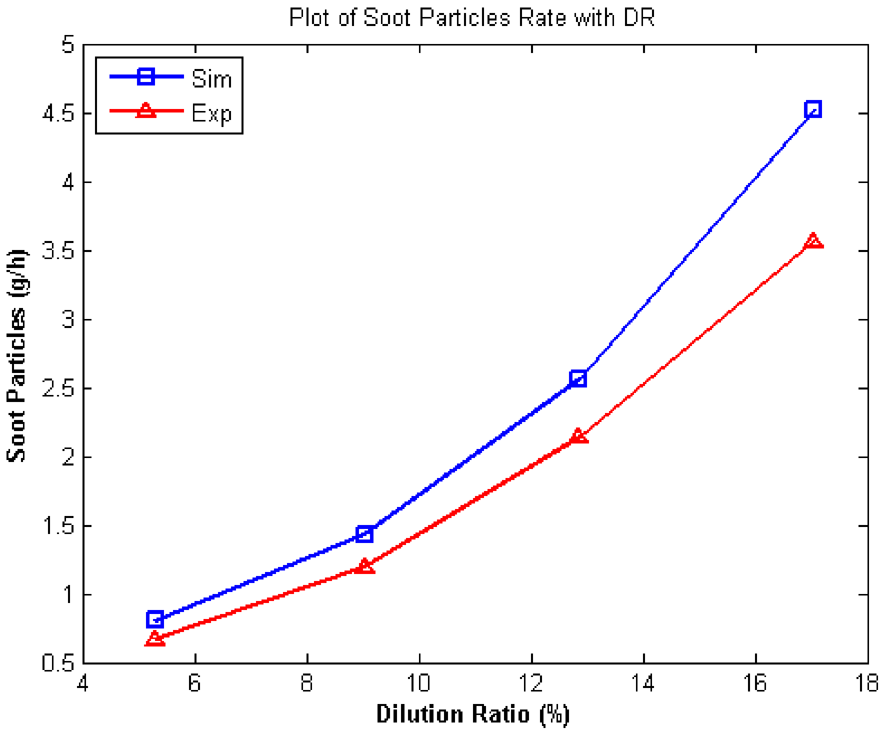

Fig. 14. Comparison of simulated and measured results with EGR and water at point B after model modification

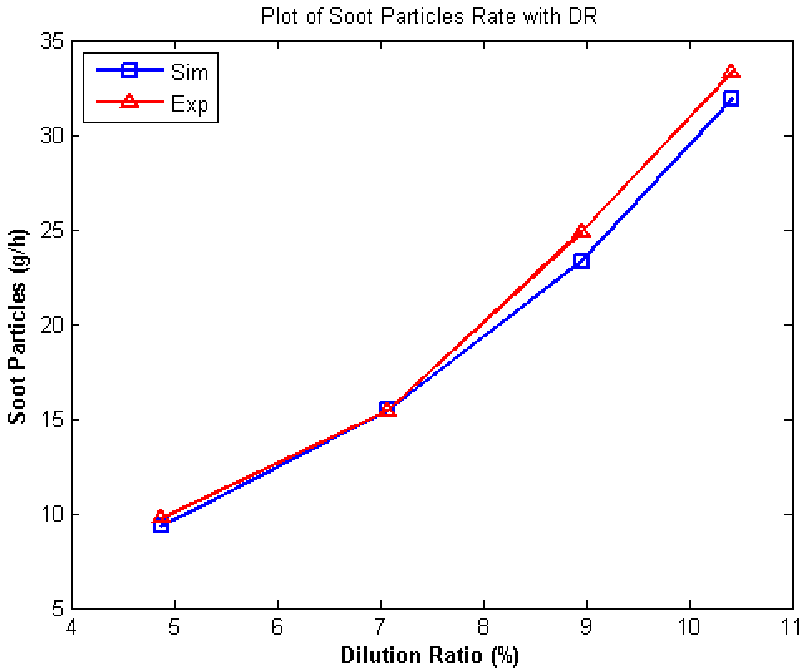

Fig. 15. Comparison of simulated and measured results with EGR and water at point C after model modification

10.4. Results with water injection

The amount of water injected and the dilution ratios for points B and C are shown in table 08.

Table 08: Dilution ratios and amount of water at point B and C

Test Point	DR (%)	$\dot{m}_w$ (g/h)	m_w (mg)
B	2.968	3	16.4
	4.705	5	25.8
	6.551	7	35.7
	8.256	9	44.5
C	1.74	3	13.4
	2.692	5	20.7
	4.01	7	30.7
	4.964	9	37.8

Here, the values of n_2 used are 0.7 and 1 depending on the ratio $(\frac{\dot{m}_w}{\dot{m}_f})$. When the model was applied for the cases with water injection at point B and point C the following plots were obtained as shown in fig.16 and fig.17.

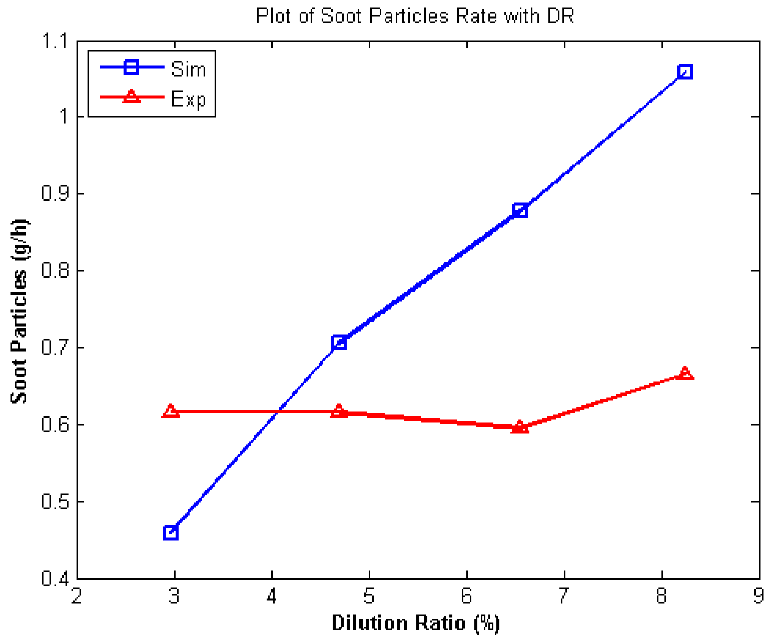

Fig. 16. Comparison of simulated and measured results with water at point B after model modification

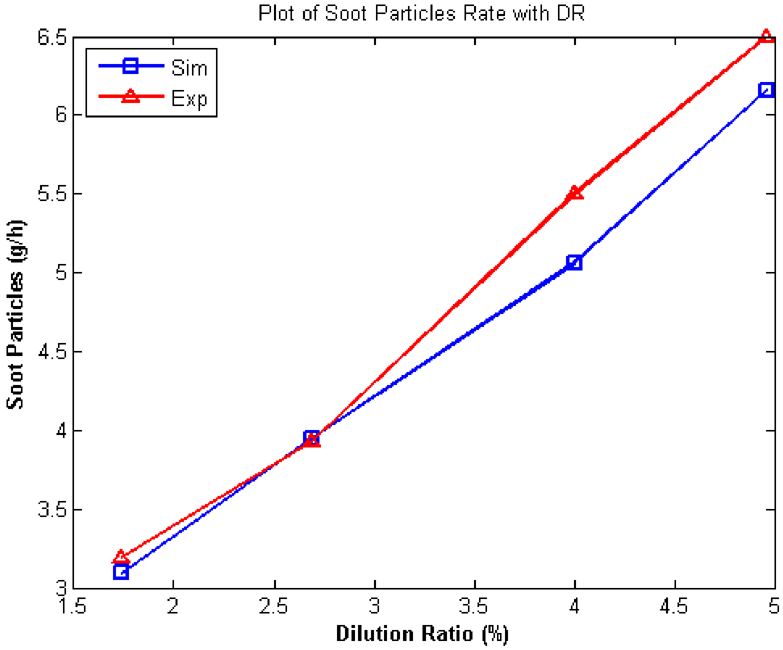

Fig.17. Comparison of simulated and measured results with water at point C after model modification

As expected the results for point B showed errors. The measured soot results showed a decrease whereas the modeled soot was increasing. This is because when water is injected in the chamber the combustion becomes unstable. When the amount of water is increased little or no combustion happens due to lower loading conditions and thus the net soot produced is lowered. In comparison, the model shows an increase due to the exponential terms involved.

The case for point C is different. As the amount of air and fuel are more than point B, combustion happens even with the introduction of water in the chamber. But as the amount of water is increased the results start showing errors.

The results at point B and C with WI for different dilution ratios are shown in table 09.

Table 09: Soot value comparison at point B and C for WI

Test Point	DR (%)	Measured Soot (g/h)	Simulated Soot (g/h)
B	2.968	0.615	0.4591
	4.705	0.615	0.705
	6.551	0.555	0.877
	8.256	0.534	1.059
C	1.74	3.194	3.093
	2.692	3.93	3.948
	4.01	6.318	5.061
	4.964	6.863	6.158

Conclusion and Recommendations

In this research, the soot emission from diesel engine combustion has been discussed. The main idea was to understand soot formation phenomenology and to develop a predicting tool that can evaluate the quantity of soot emitted from a specific diesel engine by inputting certain parameters which are obtained experimentally. Moreover, the effects of emission reduction techniques mainly exhaust gas recirculation and water injection are also studied and then implemented in the simulation model.

The soot emissions were modeled using the two step model developed by Hiroyasu. The model showed good results with the experimental data at different loading conditions. However, the introduction of exhaust gas and water in the cylinder produced errors. This error was mainly because of the dilution affects that affect the amount of oxygen in the air. The existing Hiroyasu model is used for very simple DI diesel engines operating over a limited range. Therefore a modification is done in the existing Hiroyasu model to incorporate the effect of dilution that directly affects the formation of soot.

On comparison of the modeled results with the measured results it is evident that the modified model shows good results for different EGR rates and when EGR is used in parallel with water injection. In case of EGR only, the results are very accurate. When water is introduced in parallel, the results are accurate but as the amount of water is increased the difference between the measured and simulated results also increases. This error is more for low load point whereas for high load points the error is very small. This shows that the combustion is affected by the introduction of water.

For water injection alone, the low load point shows large errors because there is no or very little combustion happening. The high load point shows good results initially but with the increase in water quantity the error also increases.

Thus, this model can not only be used as a soot predicting tool at different loads, but it also helps in evaluating the soot quantity when EGR, water and a combination of both are used in the engine. In case of water, this model shows errors for low and moderate load points. This can help in deciding the optimum amount of exhaust gas and water quantity needed to be introduced in the chamber for minimizing the amount of soot.

For future work, there is room for improvement. The effects to combustion caused by introduction of water are not implemented in the model which is leading to error. The model can thus be improved by incorporating these affects so that it can also predict soot when water is injected at low and moderate loads. Moreover, using the experimental data a NOx production error can also be developed so that a better trade-off between and soot and NOx can be made.

References

1. Colin R. Ferguson, Allan T. Kirkpatrick, "Internal Combustion Engines Applied Thermosciences, Second Edition,"

2. Heywood, J. B., "Internal Combustion Engine Fundamentals", McGraw-Hill Book Company, 1988

3. K. Santoh, L. Zhang, H. Hatanaka, T. Takatsuki, K. Yokoto, "Relationship between NOx and SM emissions from DI diesel engine with EGR". Society of Automotive engineers of Japan, Vol.18, 1997, 369-375.

4. Zheng M, Reader GT, Hawley JG, "Diesel engine exhausts gas recirculation – a review on advanced and novel concept", Energy Conversion Management45 (2004), pp 883–900.

5. Wirbeleit, F., Enderle, C., Lehner, W., Raab, A., Binder, K., "Stratified diesel fuel-water-diesel fuel injection combined with EGR – the most efficient in-cylinder NOx and PM reduction strategy", SAE paper 972962, 1997

6. Hountalas D.T., Mavropoulos G.C., Zannis T.C., "Comparitive evaluation of EGR, intake water injection and fuel/water emulsion as NOx reduction techniques for heavy duty diesel engines", SAE paper 2007-01-0120

7. Bertola A, Boulouchos K., Li R., "Influence of water-diesel fuel emulsions of heavy duty DI diesel engines equipped with common rail injection system", SAE paper 2003-01-3146

8. Nazha M.A., Rajakaruna H., Wagstaff S.A., "The use of emulsion, water induction and EGR controlling diesel engine emissions", SAE paper 2001-01-1941

9. Hountalas D.T., Mavropoulos G.C., Binder K.B., "Effect of EGR temperature for various EGR rates on heavy duty DI diesel engine performance and emissions", Proc. 19th International Conference on Efficiency, Cost, Optimization, Simulation and Environmental Impact of Energy Systems (ECOS 2006), Vo. 2 pp-1071-1079, Crete, Greece, 12-14 July,2006.

10. Ian M. Kennedy , "Models of soot formation and oxidation', Prog. Energy Combust. Sci. Vol. 23, pp. 95-132, 1997

11. Hiroyasu H. and Kadota, T., "Models for Combustion and Formation of Nitric Oxide and Soot in DI Diesel Engines," SAE Paper 760129, 1976.

12. Hiroyasu H., Kadota, T., Development and Use of a Spray Combustion Modeling to Predict Diesel Engine Efficiency and Pollutant Emissions – Part 1 Combustion Modeling, Bulletinof the JSME, Vol. 26, No. 214, 1983

13. Desantes JM, Galindo J, Guardiola C, Dolz V., "Air mass flow estimation in turbocharged diesel engine from in-cylinder pressure measurement", Experimental Thermal and Fluid Science34 (2010), pp: 37–47.

14. Wagner RM, Green Jr JB, Dam TQ, Edwards KD, Storey JM., "Simultaneous low engine-out NOx and particulate matter with highly diluted diesel combustion", SAE (2003) Technical paper no: 2003-01-0262.

15. Bai Y-L, Wang Z, Wang J-X., "Part load characteristics of direct injection spark ignition engine using exhaust gas trap", Applied Energy87 (2010), pp 2640–2646.

16. Fontana G, Galloni E., "Experimental analysis of a spark ignition engine using exhaust gas recycle at WOT operation", Applied Energy 87 (2010), pp 2187–2193.

17. Wade RW., "Light duty NOx-HC particulate trade-off", SAE (1980), Technical paper No. 800335.

18. Needham JR, Doyle DM., "The low NOx truck engine", SAE (1991), Technical paper No., 910731.

19. Agarwal AK, Singh SK, Sinha S, Shukla MK., "Effect of EGR on the exhaust gas temperature and exhaust opacity in compression ignition engines", Sadhana 29 (2004), pp.275–284.

20. Mehta S, Oey F, Sumbung CL, Levendis YA., "An aerodynamically regenerated diesel particulate trap with a flow-through soot incinerator section", JSAE(1994) Technical paper No. 940461.

21. Cinar C, Topgul T, Ciniviz M, Hasimoglu C., "Effects of injection pressure and intake CO2 concentration on performance and emission parameters of an IDI turbocharged diesel engine", Applied Thermal Engineering 25 (2005), pp .1854–1862.

22. Dec J.E., "Advanced compression ignition engines-understanding the in-cylinder processes", Proceedings of Combustion Institute 32 (2009), pp.2727–2742.

23. Ladommatos N, Balian R, Horrocks R, Cooper L., "The effect of exhaust gas recirculation on soot formation in a high-speed direct-injection diesel engine", SAE (1996.), Technical paper no: 960841.

24. J. Hussain , K. Palaniradja, N. Algumurthi, "Effect of exhaust gas recirculation on emission characteristic of three cylinder compression ignition engine using staged combustion", Journal of Engineering Research and Studies E-ISSN0976-7916

25. Samiur R. S., "ETUDE EXPERIMENTALE ET THERMODYNAMIQUE DE L'INJECTION D'EAU A L'ADMISSION D'UN MOTEUR DIESEL AUTOMOBILE POUR LA REDUCTION A LA SOURCE DES EMISSIONS POLLUANTES" (EXPERIMENTAL AND THERMODYNAMIC STUDY OF WATER INTAKE INJECTION DIESEL ENGINE MOTOR FOR REDUCING THE SOURCE OF EMISSIONS), Ecole Centrale de Nantes (Central School of Nantes), Thèse de Doctorat, 21-10- 2011

26. Guillet, R. "Du diagramme hygrométrique de combustion aux pompes à vapeur d'eau", Elsevier 1998

27. Ladommatos, N., Abdelhalim, S. M., Zhao, H., Hu, Z., "The dilution, chemical and thermal effects of Exhaust Gas Recirculation on Diesel Engine emissions – Part 4: Effects of Carbon Dioxide and Water Vapour", SAE paper 971660, 1997

28. Samec, N., Dibble, R.W, Chen, J.H., Pagon, A. "Reduction of NOx and Soot Emission by Water Injection During combustion in a diesel engine", FISITA Automotive Congress paper F2000A075, 2000

29. Roberts, C.E., Naegeli, D., Chadwell, C., "The effect of water on soot formation", SAE paper 2005-01-3850, 2005

30. Xander J. L. S.," Development and validation of a phenomenological diesel engine combustion model", Eindhoven University of Technology

31. Tree, D. L., Svensson, K. I., "Soot processes in Compression Ignition engines", Elsevier Sciencedirect Progress in Energy and Combustion Science, 2006.

32. Kouremenos, D. A., Rakopoulos, C. D., Hountalas, D., Kotsiopoulos, P., "Forschung im Ingenieurwesen 56", 22-32 (1990).

33. Flynn, P. F., Durrett, R. P., Hunter, G. L., zur Loye, A. O., Akinyemi, O. C., Dec, J. E., Westbrook, C. K., "Diesel Combustion: An integrated view combining, Laser diagnostics, chemical kinetics, and empirical validation", SAE Paper 1999-01-0509, 1999

34. Dec, J.E., A conceptual model of DI diesel combustion based on laser-sheet imaging, SAE paper 970873, 1997

35. Siebers, D. L., Pickett, L. M., "Soot in diesel fuel jets: effects of ambient temperature, ambient density and injection pressure", Elsevier Sciencedirect Combustion and Flame, 2004.

Matlab Code

```
%%4 6 7 9 10 11%%
%%4%%
clear all
clc
press=importdata('D:\MS\Thesis\code\test paper\test\EGR12D.mat');
press2=importdata('D:\MS\Thesis\code\test paper\test\EGR13D.mat');
press3=importdata('D:\MS\Thesis\code\test paper\test\EGR14D.mat');
press4=importdata('D:\MS\Thesis\code\test paper\test\EGR15D.mat');
CR=18;
B=0.085;
S=0.088;
Vs=(pi/4)*S*B^2;
Vc=Vs/(CR-1);
R=287;
l=0.152;
r=S/2;
n=l/r;
inj_ip=19.05;
inj_dp=2.34;
inj_im=0.42;
inj_dm=11.62;
% inj_d=inj_i+inj_e;
% inj_mid=inj_d/2;
P_man=1.156e+5;
step=0.36;
rpm=1997;
ww=12*pi*rpm;
aflow=184.8/3600;             %178.7 177.6 177.3 176 WI
                              %179.6 171.4 165.4 160.5EGR
                              %171.6 165.4 160.6 155.8 WI EGR


aflowm=[179.6 171.4 165.4 160.5]/3600;
t_air=180/(rpm*6);
% t_fuel=inj_d/(rpm*6);
vel=S*rpm/30;
lambda=1;
DR=[1.65 4.18 6.76 8.089];           %3.19 3.93 6.31 6.86PM  %1.74 2.69 4
4.964DR WI
                                     %2.96 6.4 13.74 19.26PM  %1.65 4.18
6.76 8.089DR EGR
                                     %9.75 15.4 24.85 33.3PM  %4.875 7.08
8.957 10.419DR WI            %EGR
Oxy_conc_m=22.318;
mw=[0 0 0 0]; %rate                  %3.3 5.2 7.1 8.9
fmf=9.64;

omg=1.4*rpm/1750;
tor=200/320;
fact=omg*tor*exp(0.285*DR(1));
fact2=omg*tor*exp(0.285*DR(2));
fact3=omg*tor*exp(0.285*DR(3));
fact4=omg*tor*exp(0.285*DR(4));

% fact=1;
% fact2=1;
% fact3=1;
```

```
% fact4=1;

for j=1:1:1

%%CYLINDER VOLUME%%
for i=1:1:720/step
        V(i)= Vs*((CR-1)^(-1)+(0.5)*(n+1-cos((i*step)*pi/180)-(n^2-
(sin((i*step)*pi/180))^2)^0.5));
        ss(i)=r*(1+n-cos(i*step*pi/180)-((n)^(2)-
(sin(i*step*pi/180))^(2))^0.5);
        a(i)=Vs*0.5*sin(i*step*pi/180);
    b(i)=(cos(i*step*pi/180))*((n^(2)-(sin(i*step*pi/180))^2)^-0.5);
    dvv(i)=a(i)*(1+b(i));
end
%     plot (dvv)
for i=500:1:1500
    vv(i)=V(i);
    s(i)=ss(i);
end

for i=500:1:1499
    dv(i)=(vv(i+1)-vv(i));
    dvn(i)=dvv(i);
end
% plot (dvn);

%%Pressure%%
P=press(:,4);
P2=press2(:,4);
P3=press3(:,4);
P4=press4(:,4);
for i=500:1:1500
    pp(i)=P(i+229);
     pp2(i)=P2(i+229);
     pp3(i)=P3(i+229);
     pp4(i)=P4(i+229);
end
  Rp=1; Rs=200;
Ws=0.0009/2; Wp=0.5;
[NN,Wn] = buttord(Wp, Ws, Rp, Rs);
[Z,A] = butter(NN,Wn);
PP = filter(Z,A,pp);
PP2 = filter(Z,A,pp2);
PP3 = filter(Z,A,pp3);
PP4 = filter(Z,A,pp4);
% plot (PP)
% hold on
% plot (PP2)
% hold on
% plot (PP3)
% hold on
% plot (PP4)
%%Mixture Mass%%
mair=aflow*t_air;
mairm=aflowm*t_air;
mfp=0.0000024;
mfm=0.0000397;
mft=mfp+mfm;
ubhc=0.8/1000;
dmair=mair/(180/step);
```

```
% mf=fflow*t_fuel;
dmfp=mfp/(inj_dp/step);
dmfm=mfm/(inj_dm/step);
mf(1)=0;
mmix(1)=0;
for i=1:1:180/step
    mmix(i+1)=mmix(i)+dmair;
    mf(i)=0;
    mff(i)=0;
end

for i=180/step:1:round((360-inj_ip)/step)
    mmix(i+1)=mmix(i);
    mf(i)=0;
    mff(i)=0;

end

for i=round((360-inj_ip)/step):1:round((360-inj_ip+inj_dp)/step)
    mmix(i+1)=mmix(i)+(1*dmfp);
    mf(i+1)=dmfp;
    mff(i+1)=mff(i)+dmfp;

end
for i=round((360-inj_ip+inj_dp)/step):1:round((360-inj_im)/step)
    mmix(i+1)=mmix(i);
    mf(i+1)=0;
    mff(i+1)=mff(i);
end

for i=round((360-inj_im)/step):1:round((360-inj_im+inj_dm)/step)
    mmix(i+1)=mmix(i)+dmfm;
    mf(i)=dmfm;
    mff(i+1)=mff(i)+dmfm;
end
for i=round((360-inj_im+inj_dm)/step):1:1500
    mmix(i+1)=mmix(i);
    mf(i)=0;
    mff(i+1)=mff(i);
end
% plot (mff)
for i=500:1:1500
    m(i)=mmix(i);
    mmf(i)=mf(i);
    mmff(i)=mff(i);
end
% plot (mmix)


%%%%TEST TEMP%%%
for i=500:1:1500
Ttest(i)=(PP(i)*100000*V(i))/(mmff(i)+mair)/R;
Ttest2(i)=(PP2(i)*100000*V(i))/(mmff(i)+mair)/R;
Ttest3(i)=(PP3(i)*100000*V(i))/(mmff(i)+mair)/R;
Ttest4(i)=(PP4(i)*100000*V(i))/(mmff(i)+mair)/R;
% plot (Ttest)
% hold on
% plot (Ttest2)
% hold on
% plot (Ttest3)
```

```
% hold on
% plot (Ttest4)

 lambda(i) = mair/mmf(i)/14.7;
 if (Ttest(i)>600)
    cp(i)=(166.3+24.5/lambda(i))*log(Ttest(i)-70-120/lambda(i));
    cp2(i)=(166.3+24.5/lambda(i))*log(Ttest2(i)-70-120/lambda(i));
    cp3(i)=(166.3+24.5/lambda(i))*log(Ttest3(i)-70-120/lambda(i));
    cp4(i)=(166.3+24.5/lambda(i))*log(Ttest4(i)-70-120/lambda(i));
else
    if(lambda(i)<8)
        cp(i)=(975.5+0.28*Ttest(i))-((11.92+0.06*Ttest(i))*log(lambda(i)));
         cp2(i)=(975.5+0.28*Ttest2(i))-
((11.92+0.06*Ttest2(i))*log(lambda(i)));
          cp3(i)=(975.5+0.28*Ttest3(i))-
((11.92+0.06*Ttest3(i))*log(lambda(i)));
           cp4(i)=(975.5+0.28*Ttest4(i))-
((11.92+0.06*Ttest4(i))*log(lambda(i)));
    else
        cp(i)=1000+2.85*exp((Ttest(i)-273.15)/100*0.88);
        cp2(i)=1000+2.85*exp((Ttest2(i)-273.15)/100*0.88);
        cp3(i)=1000+2.85*exp((Ttest3(i)-273.15)/100*0.88);
        cp4(i)=1000+2.85*exp((Ttest4(i)-273.15)/100*0.88);
    end

end
cv(i)=cp(i)-R;
cv2(i)=cp2(i)-R;
cv3(i)=cp3(i)-R;
cv4(i)=cp4(i)-R;
gamma(i)= (cp(i))/(cv(i));
end
% plot (cp)
Rp=1; Rs=200;
Ws=0.0009/2; Wp=0.5;
[NN,Wn] = buttord(Wp, Ws, Rp, Rs);
[Z,A] = butter(NN,Wn);
T_test = filter(Z,A,Ttest);


%%%dT%%%%
for i=500:1:1499
    dT(i)=(Ttest(i+1)-Ttest(i));
    dT2(i)=(Ttest2(i+1)-Ttest2(i));
    dT3(i)=(Ttest3(i+1)-Ttest3(i));
    dT4(i)=(Ttest4(i+1)-Ttest4(i));
    end

%%Heat Transfer%%
for i=500:1:1500
    Ar(i)=(pi/2)*B^(2) + pi*B*s(i);
    h(i)=130*(vv(i)^-(0.06))*((PP(i))^(0.8))*(Ttest(i)^(-
0.4))*(vel+1.4)^(0.8);
    h2(i)=130*(vv(i)^-(0.06))*((PP2(i))^(0.8))*(Ttest2(i)^(-
0.4))*(vel+1.4)^(0.8);
    h3(i)=130*(vv(i)^-(0.06))*((PP3(i))^(0.8))*(Ttest3(i)^(-
0.4))*(vel+1.4)^(0.8);
    h4(i)=130*(vv(i)^-(0.06))*((PP4(i))^(0.8))*(Ttest4(i)^(-
0.4))*(vel+1.4)^(0.8);
    hloss(i)=(h(i)*Ar(i)*(Ttest(i)-450))/6/rpm;
```

```
     hloss2(i)=(h2(i)*Ar(i)*(Ttest2(i)-450))/6/rpm;
      hloss3(i)=(h3(i)*Ar(i)*(Ttest3(i)-450))/6/rpm;
       hloss4(i)=(h4(i)*Ar(i)*(Ttest4(i)-450))/6/rpm;

end
% plot (hloss)

%%%%ROHR%%%%
for i=500:1:1499
dW(i)= PP(i)*100000*dv(i);
dU(i)=(mmf(i)+mairm(1))*cv(i)*dT(i);
dQ(i)=dU(i)+dW(i);
dQQ(i)=dU(i)+dW(i)-hloss(i);
dW2(i)= PP2(i)*100000*dv(i);
dU2(i)=(mmf(i)+mairm(2))*cv2(i)*dT2(i);
dQ2(i)=dU2(i)+dW2(i);
dQQ2(i)=dU2(i)+dW2(i)-hloss2(i);
dW3(i)= PP3(i)*100000*dv(i);
dU3(i)=(mmf(i)+mairm(3))*cv3(i)*dT3(i);
dQ3(i)=dU3(i)+dW3(i);
dQQ3(i)=dU3(i)+dW3(i)-hloss3(i);
dW4(i)= PP4(i)*100000*dv(i);
dU4(i)=(mmf(i)+mairm(4))*cv4(i)*dT4(i);
dQ4(i)=dU4(i)+dW4(i);
dQQ4(i)=dU4(i)+dW4(i)-hloss4(i);
% dQ(i)=dU(i)+dW(i)-hloss(i);
end
% plot (dQQ)
% hold on
% plot (dQQ2)
% hold on
% plot (dQQ3)
% hold on
% plot (dQQ4)
Rp=1; Rs=3000;
Ws=0.0009/2; Wp=0.5;
[NN,Wn] = buttord(Wp, Ws, Rp, Rs);
[Z,A] = butter(NN,Wn);
d_Q = filter(Z,A,dQ);
d_Q2 = filter(Z,A,dQ2);
d_Q3 = filter(Z,A,dQ3);
d_Q4 = filter(Z,A,dQ4);

% plot (d_Q)

%%%CHOR%%%
dQt(500)=0;
dQt2(500)=0;
dQt3(500)=0;
dQt4(500)=0;

for i=500:1:1498
    dQt(i+1)=dQt(i)+d_Q(i);
    dQt2(i+1)=dQt2(i)+d_Q2(i);
    dQt3(i+1)=dQt3(i)+d_Q3(i);
    dQt4(i+1)=dQt4(i)+d_Q4(i);

end
% plot (dQt)
```

```
%%%air burnt%%%
HC=4.27e7;

for i=500:1:1498
   mb(i)=dQt(i)/HC;
    mb2(i)=dQt2(i)/HC;
     mb3(i)=dQt3(i)/HC;
      mb4(i)=dQt4(i)/HC;
  end
for i=970:1:1498
      mub(i)=mmff(i)-mb(i);
       mub2(i)=mmff(i)-mb2(i);
        mub3(i)=mmff(i)-mb3(i);
         mub4(i)=mmff(i)-mb4(i);
    if mub(i)<0
        mub(i)=0;
    end
    if mub2(i)<0
        mub2(i)=0;
    end
    if mub3(i)<0
        mub3(i)=0;
    end
    if mub4(i)<0
        mub4(i)=0;
    end
end
% plot (mub)

%%Partial Pressure of Oxygen%%
% mf=fflow*t_fuel;
HC=4.27e+7;
Qinp=mfp*HC;
Qinm=mfm*HC;
Qin=mft*HC;
frm=1;
a=17.75+(3.825*frm)-(4.575*frm^2);
n=2.5+(2.125*frm)-(.125*frm^2);

for i=1:1:round((360-inj_ip)/step)
    nn(i)=1;
end
for i=round((360-inj_ip)/step):1:round((360-inj_ip+inj_dp)/step)
    f(i)=(1-exp(-a*((i-round((360-
inj_ip)/step))/round((inj_dp)/step))^n))*0.063;
%      df(i)=((n*a)/inj_dp/step)*(1-f(i))*((i-((360-
inj_ip))/step)/(inj_dp)/step)^(n-1);
        nn(i)=1-f(i);
end
%  plot (f)
for i=round((360-inj_ip+inj_dp)/step):1:round((360-inj_im)/step)
    f(i)=0.063;
    nn(i)=0.937;
%     df(i)=0;
end
%  plot (f)
for i=round((360-inj_im)/step):1:round((360-inj_im+inj_dm)/step)
   f(i)=(1-exp(-0.06213-a*((i-round((360-
inj_im)/step))/round((inj_dm)/step))^n));
    nn(i)=1-f(i);
```

```
%      df(i)=((n*a)/inj_dm/step)*(1-f(i))*((i-((360-
inj_im))/step)/(inj_dm)/step)^(n-1);
 end
% plot (f)
for i=round((360-inj_im+inj_dm)/step):1:1500
   f(i)=1;
   nn(i)=0;
%    df(i)=0;
end


for i=500:1:1500
    ff(i)=f(i);
    po(i)=nn(i);
end
for i=500:1:1499

    df(i)=(ff(i+1)-ff(i));
end
% plot (df)

P_amb=100000;
Oxy_conc=Oxy_conc_m-(Oxy_conc_m*DR(1)*0.01);%percent
Oxy_conc2=Oxy_conc_m-(Oxy_conc_m*DR(2)*0.01);
Oxy_conc3=Oxy_conc_m-(Oxy_conc_m*DR(3)*0.01);
Oxy_conc4=Oxy_conc_m-(Oxy_conc_m*DR(4)*0.01);

for i=500:1:1500
ppo(i) = 0.01*Oxy_conc*P_amb*po(i);
ppo2(i) = 0.01*Oxy_conc2*P_amb*po(i);
ppo3(i) = 0.01*Oxy_conc3*P_amb*po(i);
ppo4(i) = 0.01*Oxy_conc4*P_amb*po(i);
end

% %%Soot Formation%%

xx=1:1:1498;
xx2=1:1:1500;
yy=xx*step;
yy2=xx2*step;
P_amb=100000;
Oxy_conc_amb=21;
Act_ef=52250;
Act_eb=58520;
RR=8314;

Af=0.0075;
Ab=0.0005;

soott(round((360-inj_ip)/step))=0;
soott2(round((360-inj_ip)/step))=0;
soott3(round((360-inj_ip)/step))=0;
soott4(round((360-inj_ip)/step))=0;

 for i=round((360-inj_ip)/step):1:1498

 a1(i)=exp(-Act_ef/RR/Ttest(i));
 b1(i)=exp(-Act_eb/RR/Ttest(i));
 a2(i)=exp(-Act_ef/RR/Ttest2(i));
```

```
 b2(i)=exp(-Act_eb/RR/Ttest2(i));
 a3(i)=exp(-Act_ef/RR/Ttest3(i));
 b3(i)=exp(-Act_eb/RR/Ttest3(i));
 a4(i)=exp(-Act_ef/RR/Ttest4(i));
 b4(i)=exp(-Act_eb/RR/Ttest4(i));

 sootf(i)=Af*(mub(i)*fact)*1000*((PP(i))^0.5)*a1(i);
 soott(i+1)=soott(i)+sootf(i);
 sootb(i)=Ab*soott(i)*ppo(i)*(PP(i)^(.8))*b1(i)/100000;
 sootn(i)=((sootf(i)-sootb(i))*3600);
 sootft(i)=(Af*(mub(i)*fact)*1000*((PP(i))^0.5)*a1(i))/ww;
 sootbt(i)=(Ab*sootft(i)*ppo(i)*(PP(i)^(.8))*b1(i))/100000/ww;
 sootnt(i)=(sootft(i)-sootbt(i));

 sootf2(i)=Af*(mub2(i)*fact2)*1000*((PP2(i))^0.5)*a2(i);
 soott2(i+1)=soott2(i)+sootf2(i);
 sootb2(i)=Ab*soott2(i)*ppo2(i)*(PP2(i)^(.8))*b2(i)/100000;
 sootn2(i)=((sootf2(i)-sootb2(i))*3600);
 sootft2(i)=(Af*(mub2(i)*fact2)*1000*((PP2(i))^0.5)*a2(i))/ww;
 sootbt2(i)=(Ab*sootft2(i)*ppo2(i)*(PP2(i)^(.8))*b2(i))/100000/ww;
 sootnt2(i)=(sootft2(i)-sootbt2(i));

 sootf3(i)=Af*(mub3(i)*fact3)*1000*((PP3(i))^0.5)*a3(i);
 soott3(i+1)=soott3(i)+sootf3(i);
 sootb3(i)=Ab*soott3(i)*ppo3(i)*(PP3(i)^(.8))*b3(i)/100000;
 sootn3(i)=((sootf3(i)-sootb3(i))*3600);
 sootft3(i)=(Af*(mub3(i)*fact3)*1000*((PP3(i))^0.5)*a3(i))/ww;
 sootbt3(i)=(Ab*sootft3(i)*ppo3(i)*(PP3(i)^(.8))*b3(i))/100000/ww;
 sootnt3(i)=(sootft3(i)-sootbt3(i));

 sootf4(i)=Af*(mub4(i)*fact4)*1000*((PP4(i))^0.5)*a4(i);
 soott4(i+1)=soott4(i)+sootf4(i);
 sootb4(i)=Ab*soott4(i)*ppo4(i)*(PP4(i)^(.8))*b4(i)/100000;
 sootn4(i)=((sootf4(i)-sootb4(i))*3600);
 sootft4(i)=(Af*(mub4(i)*fact4)*1000*((PP4(i))^0.5)*a4(i))/ww;
 sootbt4(i)=(Ab*sootft4(i)*ppo4(i)*(PP4(i)^(.8))*b4(i))/100000/ww;
 sootnt4(i)=(sootft4(i)-sootbt4(i));

 end
end
Rp=1; Rs=200;
Ws=0.0009/2; Wp=0.5;
[NN,Wn] = buttord(Wp, Ws, Rp, Rs);
[Z,A] = butter(NN,Wn);
sootnf = filter(Z,A,sootn);
sootnf2 = filter(Z,A,sootn2);
sootnf3 = filter(Z,A,sootn3);
sootnf4 = filter(Z,A,sootn4);

pt2=sum(sootnf)*step/180
pt3=sum(sootnf2)*step/180
pt4=sum(sootnf3)*step/180
pt5=sum(sootnf4)*step/180

PMe=[2.96 6.4 13.74 19.26];
meas=[pt2 pt3 pt4 pt5];
plot (DR,meas,'marker','s','LineWidth',2);
hold on
plot (DR,PMe,'-r','marker','^','LineWidth',2);
xlabel('Dilution Ratio (%)','fontweight','b')
```

```
ylabel('Soot Particles (g/h)','fontweight','b')
% title('Plot of Soot Particles Rate with DR')
legend('Sim','Exp',2);


% plot (yy,sootnt,'-b','LineWidth',2);
% hold on
% plot (yy,sootnt2,'-g','LineWidth',2);
% hold on
% plot (yy,sootnt3,'-k','LineWidth',2);
% hold on
% plot (yy,sootnt4,'-r','LineWidth',2);
% legend('DR=1.65%','DR=4.18%','DR=6.76%','DR=8.089%',2);
% % title('Plot of Net Soot Rate with Crank Angle')
% xlabel('Crank Angle (deg)','fontweight','b')
% ylabel('Net Soot (g)','fontweight','b')
%
% plot (yy,sootnt,'LineWidth',2);
% % title('Plot of Net Soot Rate with Crank Angle')
% xlabel('Crank Angle (deg)','fontweight','b')
% ylabel('Soot (g)','fontweight','b')



%
% A=[0.2682 0.7 1.677];
% B=[0.225 0.61 1.76];
% C=[1,2,3];
% plot (C,A,'marker','s','LineWidth',2);
% hold on
% plot (C,B,'-r','marker','^','LineWidth',2);
% set(gca,'XTick',1:1:3);
% set(gca,'XTickLabel',{'Point A','Point B','Point C'});
% % xlabel('Points','fontweight','b')
% ylabel('Soot Particles (g/h)','fontweight','b')
% % title('Plot of Soot Particles Rate at Different Loads')
% legend('Sim','Exp',2);
% %
```